doi: 10.5028/jatm.v10.944 ORIGINAL PAPER

Synthesis of Graphene Oxide and Functionalized CNT Nanocomposites Based on Epoxy Resin

Marina Borgert Moraes[1], Luciana Cividanes[1], Gilmar Thim[1]

Moraes MB http://orcid.org/0000-0002-1384-6131
Cividanes L http://orcid.org/0000-0001-6932-8619
Thim G http://orcid.org/0000-0001-6410-3031

How to cite

Moraes MB; Cividanes L; Thim G (2018) Synthesis of Graphene Oxide and Functionalized CNT Nanocomposites Based on Epoxy Resin. J Aerosp Technol Manag, 10: e3418. doi: 10.5028/jatm.v10.944.

ABSTRACT: Lately, nanomaterials have been largely studied as reinforcements for epoxy resin. Although their usage is highly promising, the literature has reported some drawbacks regarding the improvement of mechanical properties in nanocomposites. These difficulties are usually due to dispersion of nanomaterials and its adhesion to the polymeric matrix. One approach to this problem is the functionalization of nanomaterials such as carbon nanotubes (CNTs) and graphene. In this work, we have studied the synthesis and functionalization process of CNTs and graphene oxide (GO) to be used as reinforcements for epoxy resin nanocomposites. CNTs were synthesized at 850 °C in a quartz furnace, from hexane and ferrocene vapor, and functionalized by acids and ethylenediamine treatments. GO was obtained by graphite exfoliation through a modified Hummer's method. The nanomaterials were characterized by Raman spectrum, FT-IR, XRD, and SEM images. Nanocomposites were prepared using these nanomaterials and evaluated by DMA. While both nanomaterials showed an improvement in mechanical properties, suggesting a chemical bond between nanomaterial and the epoxy matrix, it was clear that GO reinforced samples presented a higher storage modulus.

KEYWORDS: Carbon nanotubes, Graphene oxide, Functionalization, Nanocomposites, Epoxy resin.

INTRODUCTION

Epoxy resins are high performance thermoset polymers widely used in various industrial applications and largely studied as nanocomposites (Chen *et al.* 2007; Saeb *et al.* 2015). The development of nanocomposites has become of great interest in materials science, and it has attracted the attention of aeronautics industries because of its potential to reduce weight of metallic structures that can be replaced by nanocomposites (Francisco *et al.* 2015). Its superior strength-to-weight ratio can lead to the reduction of fuel consumption, which is a challenge for aerospace engineering and industry (Gohardani *et al.* 2014).

Nanomaterials are generally regarded as high potential fillers to act as reinforcements and improve mechanical properties of polymers (Gojny *et al.* 2005; Wang and Liew 2015). Carbon nanotubes (CNTs) are carbon allotropes discovered by Iijima in 1991 that have attracted great interest from both scientific and industrial communities due to its outstanding properties (Iijima 1991; Kumar *et al.* 2014). CNTs have frequently been added to polymers to increase the mechanical, electrical and thermal properties of nanocomposites. But as-grown CNTs usually present a mixture of various diameters, lengths, and chiralities,

1.Departamento de Ciência e Tecnologia Aeroespacial – Instituto Tecnológico de Aeronáutica – Divisão de Ciências Fundamentais – São José dos Campos/SP – Brazil.
Correspondence author: Marina Borgert Moraes | Departamento de Ciência e Tecnologia Aeroespacial – Instituto Tecnológico de Aeronáutica – Divisão de Ciências Fundamentais | Praça Marechal Eduardo Gomes, 50 | CEP: 12.228-904 – São José dos Campos/SP – Brazil | E-mail: marinaborgert@msn.com
Received: Jun. 28, 2017 | **Accepted:** Oct. 30, 2017
Section Editor: Mariana Fraga

as well as impurities and defects. Also, CNTs aggregation can hinder the mechanical properties of nanocomposites, making its dispersion a keynote in the manufacturing process (Disfani and Jafari 2013).

Graphene is virtually a one-atom-thick molecule, with a structure of two dimensional (2D) planar sheet of sp^2 bonded carbon; it may present extraordinary properties such as high surface area (2630 m^2g^{-1}), excellent electronic conductivity, high chemical and thermal stability, and high surface chemistry (Kumar *et al.* 2017). In practice, graphene may present more than one layer due to the difficulties to separate graphite layers and to keep them apart. Several studies about graphene deal with graphene oxide, which consists of various oxygen containing functional groups (epoxy, hydroxyl, carbonyl, etc.) attached to its surfaces and edges (Zhu *et al.* 2010). Graphene sheets, due to its two-dimensional structure and high aspect ratio, have been perceived as an ideal reinforcement for nanocomposites (Viculis *et al.* 2005; Si and Samulski 2008). According to Rafiee *et al.* (2009; 2010), graphene structure is expected to present better stress transfer from its platelets to the composite matrix during loading than CNTs.

However, for both CNTs and graphene materials, potential applications have become limited due to CNTs easy entanglement and agglomeration (large aspect ratio), and because graphene platelets tend to restack (van der Waals and strong π-π interactions) (Li *et al.* 2008; Yang *et al.* 2011). Therefore, one of the hardest challenges for the nanocomposites area is to achieve homogeneous dispersions of CNTs and graphene materials into the polymer matrix (Gojny *et al.* 2005). Also, obtaining a good interfacial interaction between filler and polymer is necessary for an effective load transfer to occur (Li *et al.* 2013).

One promising approach to address this matter is the chemical modification of the filler surface prior to its dispersion into the prepolymer (Xie *et al.* 2005; Zhu *et al.* 2003; Abdalla *et al.* 2007). Literature shows that, for CNTs, amine treatment can weaken the interactions between the tubes, resulting in a better dispersion and stronger interfacial adhesion to the matrix (Meng *et al.* 2008; Cividanes *et al.* 2013). In this work, we have synthesized and functionalized carbon nanotubes and synthesized oxidized graphene to minimize issues of entanglement and restacking in epoxy nanocomposites. Mechanical properties of the nanocomposites were analyzed by DMA.

EXPERIMENTAL

CNT SYNTHESIS AND FUNCTIONALIZATION

CNTs were synthesized via chemical vapor deposition (CVD) in a quartz furnace at 850 °C with gas flow of nitrogen (1000 sccm) carrying hexane and ferrocene vapor (16:84 %wt.) for 30 min. The tubes were grown in vertically aligned form over quartz plates positioned at the middle of the furnace. They were scraped off from the plates surfaces with the help of a stainless-steel spoon.

Then, CNTs were annealed at high temperature (1800 °C) in a graphite oven under inert atmosphere for 3 h, followed by two chemical treatments. In the first treatment, 0.9 g of CNTs were drowned in sulphuric and nitric acids (30 : 90 mL) for 20 h to promote its oxidation; the solution was sonicated for 2 h. To conclude this procedure, CNTs were filtered, washed with 500 mL of water and dried at 80 °C for 24 h. Following oxidation, the CNT sample underwent treatment with ethylenediamine (525 mL) in a condenser, kept at 110 °C and stirred at 700 rpm for 150 h. Afterwards it was filtered, washed with 500 mL of methanol and dried once more. The functionalized CNTs were then designated as CNT- Am.

GO SYNTHESIS

GO was synthesized through a modified Hummer's method (Wu *et al.* 2009): 6 g of natural graphite powder (Graphene Laboratories Inc.), 4.5 g sodium nitrate and 207 mL sulphuric acid were added in a reaction flask, kept at 10 °C, and stirred for 30 min, followed by the addition of 27 g potassium permanganate. The solution was stirred for 45 min and then 414 mL of water was added. After 12 h, 1260 mL of warm water and 45 mL oxygen peroxide (30%) were added. The suspension was filtered, washed several times and finally dried at 60 °C in a vacuum oven.

NANOCOMPOSITES FABRICATION

The epoxy resin used in this study was Araldite GY-260 (diglycidyl ether of bisphenol A, DGEBA) and the hardener was Aradur 972 (diaminodiphenylmethane, DDM), both supplied by Huntsman. Nanocomposite samples were prepared without

nanomaterials (i.e. neat epoxy resin), with GO and with CNT- Am. They all received the same amount of filling material, 0.25 %wt., and the same amount of hardener, 27 %wt.

To improve CNT- Am and GO dispersion, these fillers were each mixed with acetone through bath sonication (25 kHz) for 30 min. Then the solutions were added to warm samples of epoxy resin (65 °C) and suffered tip sonication (42 kHz) for another 30 min. The resulting mixtures were degasified at 80 °C for 24 h to eliminate acetone and avoid bubbles in the final nanocomposites. The hardener was added to each mixture and heated to 90 °C to melt down. Curing process was held in two stages: at 80 °C for 1 h and at 120 °C for 2 h, according to the manufacturer's instructions.

CHARACTERIZATION METHODS

Raman spectrum was used to show the graphitic ordering before and after functionalization treatments on CNT samples. It was acquired on a Renishaw 2000 Micro-Raman, with Ar laser (λ = 514.5 nm) and range of 500 – 3500 cm^{-1} (only first order spectrum is shown in results). XPS high-resolution spectra were obtained to determine atomic composition of CNT- Am and GO in a UNI-SPECS UHV spectrometer (5×10^{-7} Pa, hν = 1253.6 eV). FT-IR was used to characterize the presence of chemical groups on CNT- Am and GO surfaces. Infrared spectra were recorded on a Perkin-Elmer Spectrum GX, in the range of 4000 – 400 cm^{-1} with 4 cm^{-1} resolution, 12 scans and KBr pellet method. XRD analyses were acquired in a PANalyticalX'Pert PRO X-Ray Diffraction Unit with Kα1 radiation (λ = 1.5406 Å) emitted by a copper target at 1800 W (45 kV; 40 mA). DMA tests were performed by a TA Instrument (DMA 2980 model) with cured samples in dual cantilever mode, with 20 µm amplitude, 1 Hz frequency and 0.56 N m torque.

RESULTS AND DISCUSSION

Figure 1 shows SEM images of CNTs as grown by CVD process and after functionalisation treatments (CNT- Am). CNTs as-grown were vertically aligned, presenting large blocks of tubes. As a result of functionalisation, CNT- Am showed a slight degree of tangling, but the blocks were clearly undone and the basic structure of the tubes was preserved.

(a) (b)

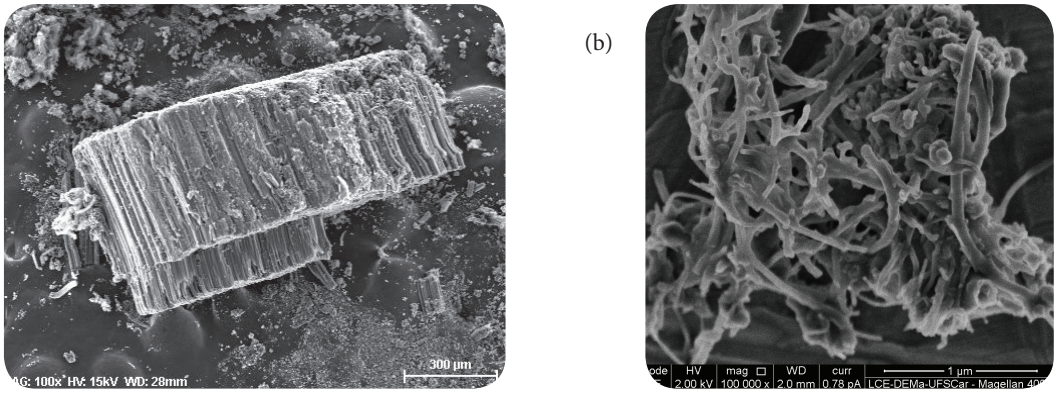

Figure 1. SEM images of CNT: (a) a block of vertically aligned CNT as grown; (b) CNT- Am after acids and ethylenediamine treatment.

Figure 2 shows the Raman spectrum of CNTs as grown and CNT- Am. CNTs as grown have clear bands at 1348.91 cm^{-1} (D band) and 1575.99 cm^{-1} (G band), and a shoulder near 1591.21 cm^{-1} (D' band). After functionalization, CNT- Am presents two bands at 1350.33 cm^{-1} (D band) and 1581.96 cm^{-1} (G band) and a shoulder near 1614.64 cm^{-1} (D' band). These bands are characteristic of multi-walled CNTs (Kuan *et al.* 2005; Wang *et al.* 1998; Belin and Epron 2005). The higher intensity of the G band for CNTs as grown indicates a higher degree of graphitisation/crystallinity, while D band is typically attributed to disordered structures (defective CNTs and non-crystalline carbon) and indicates lattice distortions in the tubes (Awasthi *et al.* 2010). The change in

intensities of D and G band could be observed on the Raman spectrum of CNT- Am due to the acid and amino functionalization process. It is known that during oxidizing treatments of graphitic structures two concurring phenomena take place: the removal of amorphous carbon from the tube walls and the formation of oxygenated functional groups (Scaffaro *et al.* 2012), changing the atomic structure from C–C sp^2 to C–C sp^3. Due to this change, a displacement in the position of G band and a higher intensity of D band can be observed (Maio *et al.* 2015). Other studies have already shown that annealing treatment is effective for reduction of defects in CNTs structure, but the acid treatment eventually damages its walls (Cividanes *et al.* 2013; Huang *et al.* 2003).

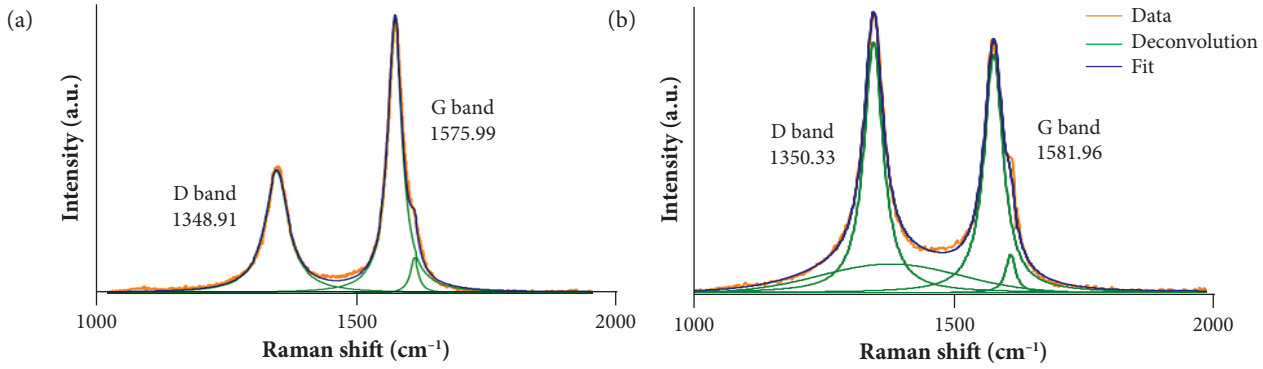

Figure 2. Raman spectrum of: (a) CNT as grown, (b) CNT- Am.

Crystallinity of carbonaceous materials can be evaluated by the ratio between D and G band intensity (I_D/I_G), as well as full width at half height (FWHM) of G band. Table 1 shows the information from the deconvoluted spectra.

Table 1. Deconvolution data of Raman spectrum of CNT as grown and CNT- Am.

Parameter	CNT as grown	CNT- Am
I_D/I_G	0.44	1.05
D band (cm^{-1})	1348.91	1350.33
G band (cm^{-1})	1575.99	1581.96
FWHM (D)	26.78	22.08
FWHM (G)	16.54	21.99

I_D/I_G ratio changed from 0.44 for CNTs as grown to 1.05 for functionalized CNT- Am. The increase in I_D/I_G ratio suggests that formation of oxygenated functional groups was more intense than removal of amorphous carbon (Scaffaro *et al.* 2012).

The presence of functional groups on CNT- Am and GO surface was confirmed by XPS analysis (Table 2). As expected, oxygen and nitrogen were found in CNT- Am, and GO exhibits high oxygen content from its oxidation. Also, exploratory scans have indicated the residual presence of sulphur and iron from growth and functionalization processes in CNT- Am (Fig. 3), as well as residual presence of sulphur in GO from its synthesis (Fig. 4).

Table 2. Atomic concentration from high resolution XPS analysis of CNT- Am and GO (± 5% precision).

Element	Atomic concentration (%)	
	CNT- Am	GO
Carbon (C1s)	94	63.8
Oxygen (O1s)	5.1	35.1
Nitrogen (N1s)	0.9	1.1

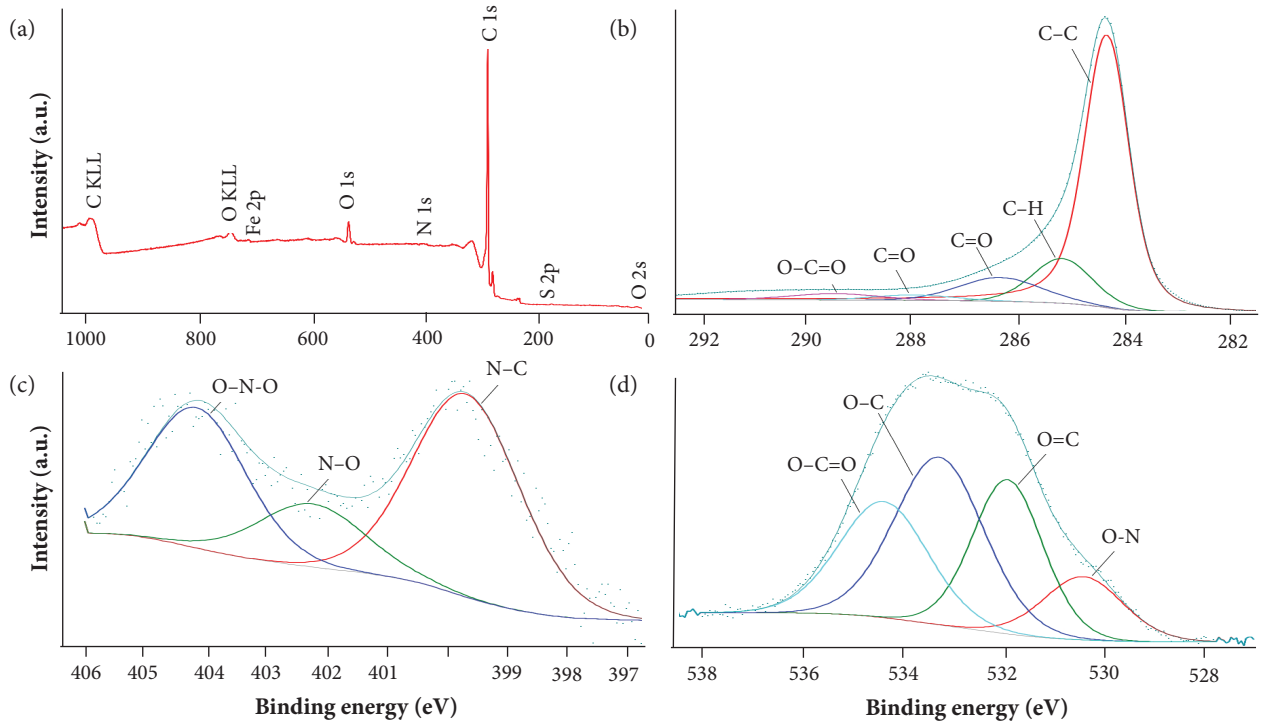

Figure 3. CNT- Am XPS scanning spectrum (a) and XPS high-resolution survey scans of: (b) C1s spectrum; (c) N1s spectrum; (d) O1s spectrum.

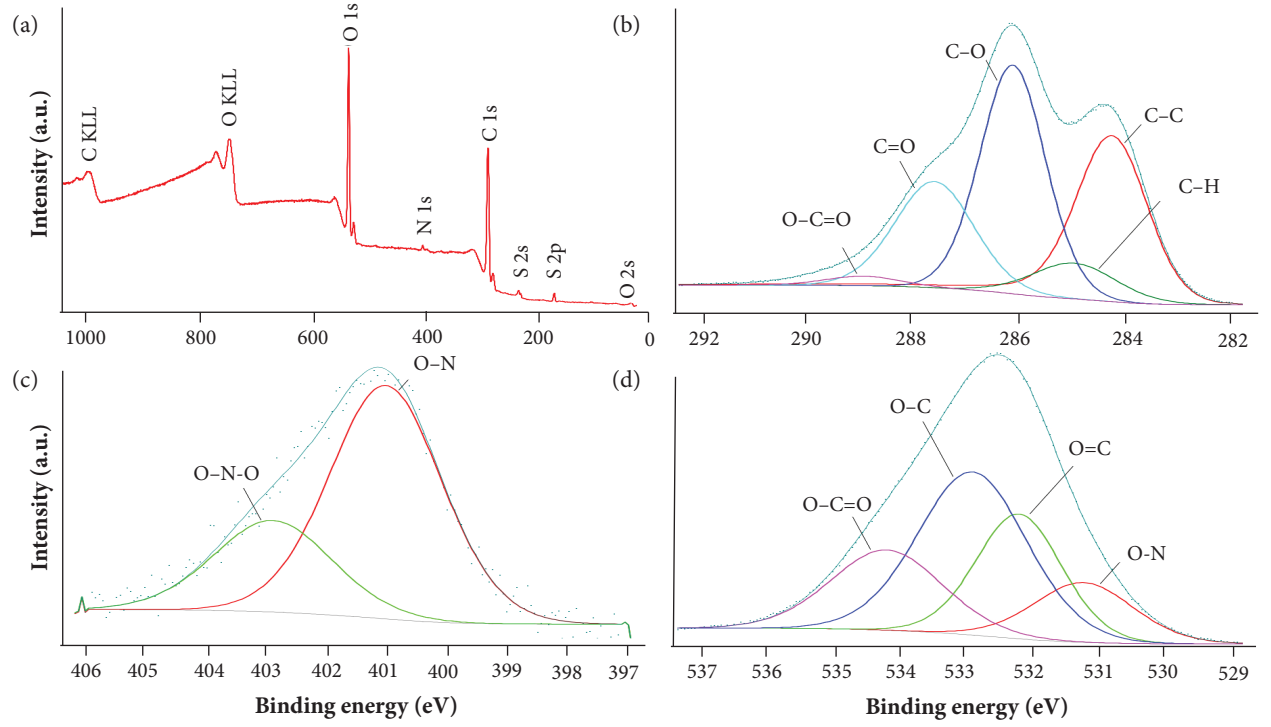

Figure 4. GO XPS scanning spectrum (a) and XPS high-resolution survey scans of: (b) C1s spectrum; (c) N1s spectrum; (d) O1s spectrum.

FT-IR analysis was used to investigate the structure and functional groups of the fillers. For CNT- Am sample (Fig. 5), FT-IR spectrum shows the following bands and peaks of interest: at 1670 cm^{-1}, corresponding to the amide carbonyl (C=O) stretching (Yang *et al.* 2007; Naumkin *et al.* 2012); at 3728 cm^{-1}, due to –NH stretching (Naumkin *et al.* 2012); at 1587 cm^{-1}, because of N–H in-plane bending (Naumkin *et al.* 2012; Xiong *et al.* 2006); and at 1220 and 1047 cm^{-1}, assigned to C–N stretching (Yang *et al.* 2007; Ma *et al.* 2010). These bands prove the presence of amide groups and lead to the conclusion that carboxylic groups on CNTs surface were modified by amine. Therefore, CNTs were indeed functionalized through the acid and amine treatments.

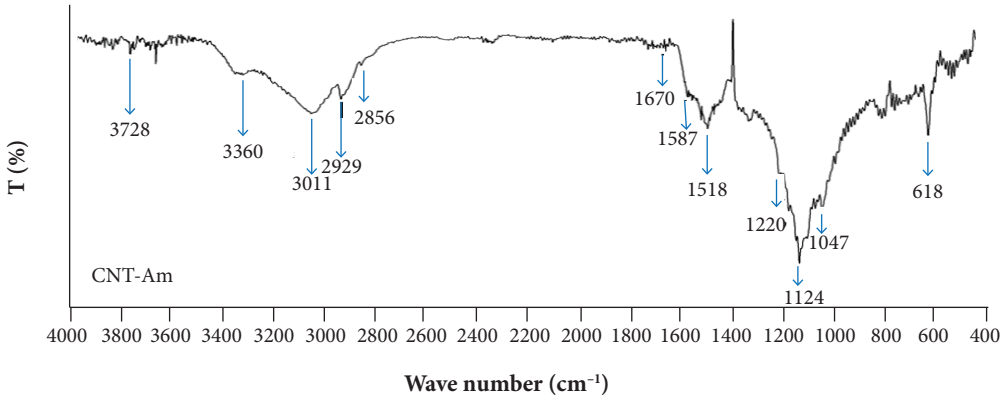

Figure 5. FT-IR spectrum of CNT- Am.

For GO sample (Fig. 6), FT-IR spectrum shows adsorption bands at 1723 cm^{-1}, due to the C=O stretch of COOH group (Song *et al.* 2014); at 1621 cm^{-1}, for stretch of C=C groups (Guo *et al.* 2009); at 1220 cm^{-1}, for C=C skeleton vibration (Thema *et al.* 2013); and at 1043 $cm^{-1}$for alkoxy C–O groups (Song *et al.* 2014). Although graphite had been oxidized into GO, C=C groups led to the conclusion that the main structure of graphite layer was retained. The presence of oxygen-containing functional groups confirmed that the graphite was greatly oxidized into GO and was in agreement with the literature (Song *et al.* 2014; Guo *et al.* 2009; Thema *et al.* 2013; Shahriary and Athawale 2014). The assignments for FT-IR spectra of CNT- Am and GO are listed on Table 3.

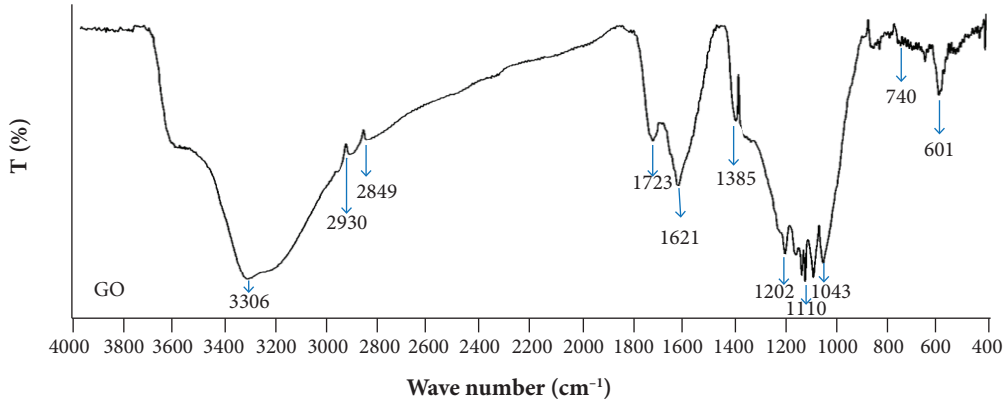

Figure 6. FT-IR spectrum of GO.

GO was characterized by XRD analysis (Fig. 7). It showed a very strong peak at $2\theta = 10.6°$, which is in accordance with those in previously reported literatures (Marcano *et al.* 2010; Fan *et al.* 2010) and corresponds to (002) crystalline plane. The peak at $2\theta = 43.3°$ corresponds to the turbostratic band of disordered carbon materials, indicating disorder between planes (101) and (012) (Zhu *et al.* 2010) and indicating that the initial graphite was not completely oxidized, which is in accordance with FT-IR results. XRD results indicated the successful synthesis of GO, although part of the original graphite remained.

Table 3. Assignments for FT-IR spectra of CNT- Am and GO.

Sample	Peak (cm^{-1})	Assignment
CNT- Am	3728	NH stretch (Awasthi *et al.* 2010)
	3360, 3296	OH stretch of COOH groups (Scaffaro *et al.* 2012)
	2945, 2929, 2856	CH stretch (Scaffaro *et al.* 2012)
	1670	C=O stretch of amide carbonyl groups (Belin and Epron 2005; Awasthi *et al.* 2010)
	1587	in plane N–H bending (Awasthi *et al.* 2010; Maio *et al.* 2015)
	1518	C=C skeleton vibration (Maio *et al.* 2015; Song *et al.* 2014)
	1220, 1047	C–N stretch (Belin and Epron 2005; Huang *et al.* 2003)
GO	3306	stretch of –OH groups from adsorbed water (Yang *et al.* 2007)
	2930	CH_2 symmetrical stretch (Naumkin *et al.* 2012)
	2849	CH_2antisymmetrical stretch (Naumkin *et al.* 2012)
	1723	C=O stretch of COOH groups (Yang *et al.* 2007)
	1635	–OH bending from adsorbed water (Ma *et al.* 2010)
	1621	C=C stretch of carbonyl groups (Naumkin *et al.* 2012)
	1385	C–O stretch of carboxylic acid groups (Naumkin *et al.* 2012)
	1220	C=C skeleton vibration (Xiong *et al.* 2006)
	1110	stretch of C–OH groups of alcohols (Naumkin *et al.* 2012)
	1043	alkoxy C–O groups (Yang *et al.* 2007)
	740	C=O stretch of carboxylic acid groups (Naumkin *et al.* 2012)

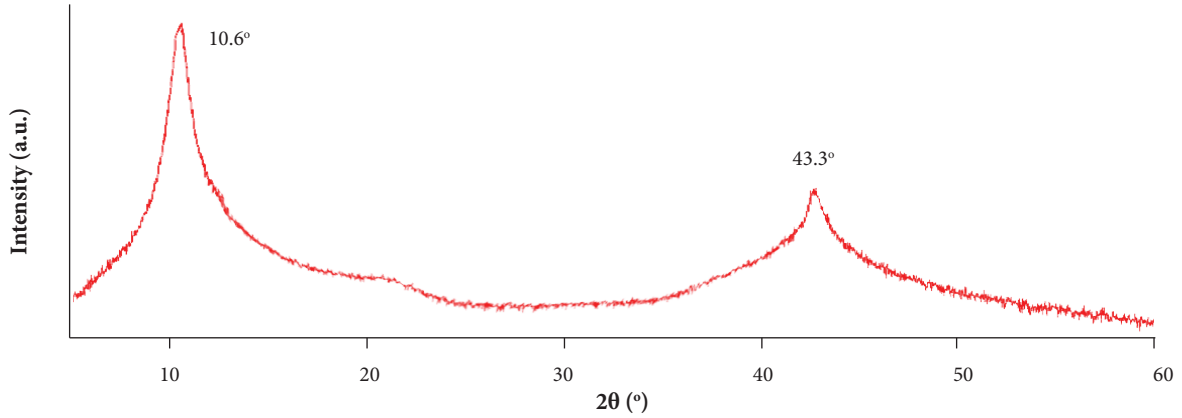

Figure 7. XRD profile of graphene GO.

Figure 8 shows the dynamic storage modulus (*E'*) versus temperature. Results showed that storage modulus decreases with temperature for all the samples. With the increase of temperature there is an increase in molecular motion of polymer chains, which decreases the polymer rigidity and hence the storage modulus (Tiwari *et al.* 2017). It is clear that mechanical strength is very dependent on the presence of CNT- Am and GO in the nanocomposites. The incorporation of CNT- Am and GO increased *E'* of the epoxy resin, both presenting some stiffening effect. This effect can be attributed to a better adhesion of the filler to the resin and to a more homogeneous dispersion (Meng *et al.* 2008). Observing glass transition temperatures (*Tg*) from loss module (*E"*) and loss tangent (tan δ) peaks, they clearly shift towards high temperature when compared to the neat resin (Table 4). *Tg* rising reflects a better adhesion to the matrix and can also be an indicator of a higher cure degree. Kalakonda and Banne (2017)

have studied the thermomechanical properties of poly(methyl methacrylate) composites reinforced with functionalized single-walled CNTs, and observed a similar increase in *Tg* for nanocomposite samples. GO nanocomposites presented a better result than CNT- Am reinforced samples, leading to the conclusion that it had a stronger interfacial adhesion with DGEBA matrix and/or more homogeneous dispersion. According to Tiwari *et al.* (2017), high surface area of GO increases the polymer nanomaterial interaction area and improve the stress transfer thus enhancing the nanocomposite storage modulus.

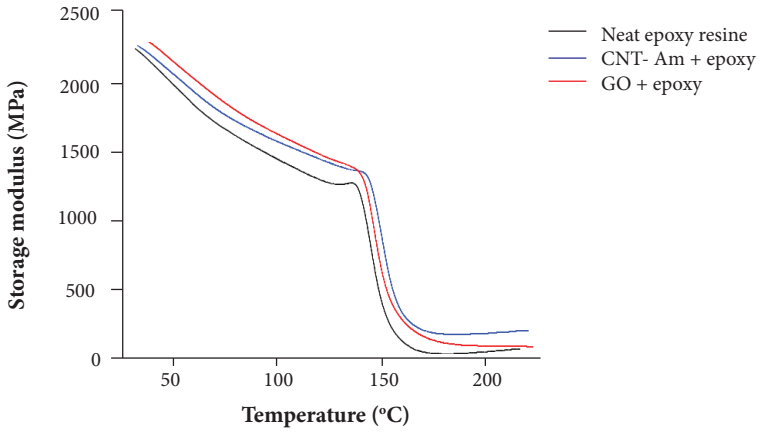

Figure 8. DMA curves of the various samples.

Table 4. Glass transition temperature (*Tg*) from loss module (*E"*) and loss tangent (tan δ) peaks.

Sample	*Tg* (°C)	
	E"	tan δ
Neat resin	137.1	160.3
CNT- Am + epoxy	147.5	165.0
GO + epoxy	149.7	166.5

CONCLUSIONS

In this study, we achieved the synthesis and functionalization of carbon nanotubes and graphene oxide. Acid and amine treatments could effectively induce polar oxygen-containing groups on CNTs surface. The modified Hummer's method successfully oxidized graphite to GO (although not completely). The morphology of functionalized CNTs was observed by SEM images and Raman spectrum. The presence of functional groups was confirmed by FT-IR and XPS spectra. These materials were studied as reinforcement fillers to DGEBA epoxy resin by dynamic mechanical analysis and effectively improved the observed mechanical properties, suggesting a chemical bond between them and the epoxy matrix. GO nanocomposite presented higher storage modulus and higher glass transition temperature than CTN-Am nanocomposite.

AUTHOR'S CONTRIBUTION

Conceptualization, Moraes MB and Thim G; Methodology, Moraes MB and Cividanes L; Investigation, Moraes MB; Writing – Original Draft, Moraes MB; Writing – Review and Editing, Moraes MB; Funding Acquisition, Moraes MB and Thim G; Resources, Moraes MB and Cividanes L; Supervision, Thim G.

ACKNOWLEDGEMENTS

The authors gratefully acknowledge FAPESP and CNPq for financial support and LAS/INPE, LEFE, and IP&D/UNIVAP for collaboration.

REFERENCES

Abdalla M, Dean D, Adibempe D, Nyairo E, Robinson P, Thompson G (2007) The effect of interfacial chemistry on molecular mobility and morphology of multiwalled carbon nanotubes epoxy nanocomposite. Polymer 48(19):5662-5670. doi: 10.1016/j.polymer.2007.06.073

Awasthi K, Kumar R, Tiwari RS, Srivastava ON (2010) Large scale synthesis of bundles of aligned carbon nanotubes using a natural precursor: turpentine oil. J ExpNanosci 5(6):498-508. doi: 10.1080/17458081003664159

Belin T, Epron F (2005) Characterization methods of carbon nanotubes: a review. Mater SciEng B 119(2):105-118. doi: 10.1016/j.mseb.2005.02.046

Chen H, Jacobs O, Wu W, Rüdiger G, Schädel B (2007) Effect of dispersion method on tribological properties of carbon nanotube reinforced epoxy resin composites. Polym Test26(3):351-360. doi: 10.1016/j.polymertesting.2006.11.004

Cividanes LS, Brunelli DD, Antunes EF, Corat EJ, Sakane KK, Thim GP (2013) Cure study of epoxy resin reinforced with multiwalled carbon nanotubes by Raman and luminescence spectroscopy. J ApplPolymSci 127(1):544-553. doi: 10.1002/app.37815

Disfani MN, Jafari S-H (2013) Assessment of intertube interactions in different functionalized multiwalled carbon nanotubes incorporated in a phenoxy resin. PolymEngSci 53(1):168-175. doi: 10.1002/pen.23244

Fan Z, Wang K, Wei T, Yan J, Song LP, Shao B (2010) An environmentally friendly and efficient route for the reduction of graphene oxide by aluminum powder. Carbon 48(5):1686-1689. doi: 10.1016/j.carbon.2009.12.063

Francisco W, Ferreira FV, Ferreira EV, Cividanes LS, Coutinho AR, Thim GP (2015) Functionalization of multi-walled carbon nanotube and mechanical property of epoxy-based nanocomposite. JAerospTechnolManag 7(3):289-293. doi: 10.5028/jatm.v7i3.485

Gohardani O, Elola MC, Elizetxea C (2014) Potential and prospective implementation of carbon nanotubes on next generation aircraft and space vehicles: a review of current and expected applications in aerospace sciences. ProgAerospSci70:42-68. doi: 10.1016/j.paerosci.2014.05.002

Gojny FH, Wichmann MHG, Fiedler B, Schulte K (2005) Influence of different carbon nanotubes on the mechanical properties of epoxy matrix composites–a comparative study. Compos Sci Technol 65(15-16):2300-2313. doi: 10.1016/j.compscitech.2005.04.021

Guo H-L, Wang X-F, Qian Q-Y, Wang F-B, Xia X-H (2009) A green approach to the synthesis of graphene nanosheets. ACS Nano 3(9):2653-2659. doi: 10.1021/nn900227d

Huang W, Wang Y, Luo G, Wei F (2003) 99.9% purity multi-walled carbon nanotubes by vacuum high-temperature annealing. Carbon 41(13):2585-2590.doi: 10.1016/S0008-6223(03)00330-0

Iijima S (1991) Helical microtubules of graphitic carbon. Nature354:56-58. doi: 10.1038/354056a0

Kalakonda P, Banne S (2017) Thermomechanical properties of PMMA and modified SWCNT composites. NanotechnolSciAppl 10:45-52. doi: 10.2147/NSA.S123734

Kuan H-C, Ma C-CM, Chang W-P, Yuen S-M, Wu H-H, Lee T-M (2005) Synthesis, thermal, mechanical and rheological properties of multiwall carbon nanotube/waterborne polyurethane nanocomposite. Compos Sci Technol 65(11-12):1703-1710. doi: 10.1016/j.compscitech.2005.02.017

Kumar R, Singh RK, Kumar P, Dubey PK, Tiwari RS, Srivastava ON (2014) Clean and efficient synthesis of graphene nanosheets and rectangular aligned-carbon nanotubes bundles using green botanical hydrocarbon precursor: sesame oil. Sci Adv Mater 6(1):76-83. doi: 10.1166/sam.2014.1682

Kumar R, Singh RK, Vaz AR, Savu R, Moshkalev SA (2017) Self-assembled and one-step synthesis of interconnected 3D network of Fe304/reduced graphene oxide nanosheets hybrid for high-performance supercapacitor electrode. ACS Appl Mater Interfaces 9(10):8880-8890. doi: 10.1021/acsami.6b14704

Li D, Müller MB, Gilje S, Kaner RB, Wallace GG (2008) Processable aqueous dispersions of graphene nanosheets. NatNanotechnol3(2):101-105. doi: 10.1038/nnano.2007.451

Li W, Dichiara A, Bai J (2013) Carbon nanotube-graphene nanoplatelet hybrids as high-performance multifunctional reinforcements in epoxy composites. Compos Sci Technol 74:221-227. doi: 10.1016/j.compscitech.2012.11.015

Ma P-C, Mo S-Y, Tang B-Z, Kim J-K (2010) Dispersion, interfacial interaction and re-agglomeration of functionalized carbon nanotubes in epoxy composites. Carbon48(6):1824-1834. doi: 10.1016/j.carbon.2010.01.028

Maio A, Fucarino R, Khatibi R, Rosselli S, Bruno M, Scaffaro R (2015) A novel approach to prevent graphene oxide re-aggregation during the melt compounding with polymers. Compos Sci Technol 119:131-137. doi: 10.1016/j.compscitech.2015.10.006

Marcano DC, Kosynkin DV, Berlin JM, Sinitskii A,Sun Z, Slesarev A, Alemany LB, Lu W, Tour JM (2010) Improved synthesis of graphene oxide. ACS Nano 4(8):4806-4814. doi: 10.1021/nn1006368

Meng H, Sui GX, Fang PF, Yang R (2008) Effects of acid- and diamine-modified MWNTs on the mechanical properties and crystallization behavior of polyamide 6. Polymer 49(2):610-620. doi: 10.1016/j.polymer.2007.12.001

Naumkin AV, Kraut-Vass A, Gaarenstroom SW, Powell CJ (2012) NIST X-ray photoelectron spectroscopy database. NIST Standard Reference Database 20:4.1. Gaithersburg: NIST.

Rafiee MA, Lu W, Thomas AV, Zandiatashbar A, Rafiee J, Tour JM, Koratkar NA (2010) Graphene nanoribbon composites. ACS Nano 4(12):7415-7420. doi: 10.1021/nn102529n

Rafiee MA, Rafiee J, Wang Z, Song H, Yu Z-Z, Koratkar N (2009) Enhanced mechanical properties of nanocomposites at low graphene content. ACS Nano 3(12):3884-3890. doi: 10.1021/nn9010472

Saeb MR, Najafi F, Bakhshandeh E, Khonakdar HA, Mostafaiyan M, Simon F, Scheffler C, Mäder E (2015) Highly curable epoxy/MWCNTs nanocomposites: an effective approach to functionalization of carbon nanotubes. ChemEng J 259:117-125. doi: 10.1016/j.cej.2014.07.116

Scaffaro R, Maio A, Agnello S, Glisenti, A (2012) Plasma functionalization of multiwalled carbon nanotubes and their use in the preparation of nylon 6-based nanohybrids. Plasma Process Polym 9(5):503-512. doi: 10.1002/ppap.201100140

Shahriary L, Athawale AA (2014) Graphene oxide synthesized by using modified Hummers approach. Int J Renew Energy Environ Eng 02(01):58-63.

Si Y, Samulski ET (2008) Synthesis of water soluble graphene. Nano Lett 8(6):1679-1682. doi: 10.1021/nl080604h

Song J, Wang X, Chang C-T (2014) Preparation and characterization of graphene oxide. Journal of Nanomaterials 2014:276143. doi: 10.1155/2014/276143

Thema FT, Moloto MJ, Dikio ED, Nyangiwe NN, Kotsedi L, Maaza M, Khenfouch M (2013) Synthesis and characterization of graphene thin films by chemical reduction of exfoliated and intercalated graphite oxide. Journal of Chemistry 2013:150536. doi: 10.1155/2013/150536

Tiwari SK,Oraon R, Adhikari AD, Nayak GC (2017) A thermomechanical study on selective dispersion and different loading of graphene oxide in polypropylene/polycarbonate blends. J ApplPolymSci 134(28):45062-45071. doi: 10.1002/app.45062

Viculis LM, Mack JJ, Mayer OM, Hahn HT, Kaner RB (2005) Intercalation and exfoliation routes to graphite nanoplatelets. J Mater Chem 15(9):974-978. doi: 10.1039/B413029D

Wang JF, Liew KM (2015) On the study of elastic properties of CNT-reinforced composites based on element-free MSL method with nanoscale cylindrical representative volume element. Compos Struct 124:1-9. doi: 10.1016/j.compstruct.2015.01.006

Wang Z, Huang X, Xue R, Chen L (1998) Dispersion effects of Raman lines in carbons. J Appl Phys 84:227-231. doi: 10.1063/1.368022

Wu Z-S, Ren W, Gao L, Liu B, Jiang C, Cheng H-M (2009) Synthesis of high-quality graphene with a pre-determined number of layers. Carbon 47(2):493-499. doi: 10.1016/j.carbon.2008.10.031

Xie X-L, Mai Y-W, Zhou X-P (2005) Dispersion and alignment of carbon nanotubes in polymer matrix: a review. Mater SciEng 49(4):89-112. doi: 10.1016/j.mser.2005.04.002

Xiong J,Zheng Z, Qin X, Li M, Li H, Wang X (2006) The thermal and mechanical properties of a polyurethane/multi-walled carbon nanotube composite. Carbon44(13):2701-2707. doi: 10.1016/j.carbon.2006.04.005

Yang L, Chen J, Wei X, Liu B, KuangY (2007) Ethylene diamine-grafted carbon nanotubes: a promising catalyst support for methanol electro-oxidation. ElectrochimActa 53(2):777-784. doi: 10.1016/j.electacta.2007.07.052

Yang S-Y, Lin W-N, Huang Y-L, Tien H-W, Wang J-Y, Ma C-CM, Li S-M, Wang Y-S (2011) Synergetic effects of graphene platelets and carbon nanotubes on the mechanical and thermal properties of epoxy composites. Carbon 49(3):793-803. doi: 10.1016/j.carbon.2010.10.014

Zhu J, Kim J, Peng H, Margrave JL, Khabashesku VN, Barrera EV (2003) Improving the dispersion and integration of single-walled carbon nanotubes in epoxy composites through functionalization. Nano Lett 3(8):1107-1113. doi: 10.1021/nl0342489

Zhu Y, Murali S, Cai W, Li X, Suk JW, Potts JR, Ruoff RS (2010) Graphene and graphene oxide: synthesis, properties, and applications. Adv Mater 22(35):3906-3924. doi: 10.1002/adma.201001068